ABSTRACT: A tissue-based approach to in vitro drug screening allows for determination of the cumulative positive and negative effects of a drug at the tissue rather than the cellular or subcellular level. Skeletal muscle myoblasts were tissue-engineered into three-dimensional muscle with parallel myofibers generating directed forces. When grown attached to two flexible microposts (μposts) acting as artificial tendons in a 96-well plate format, the miniature bioartificial muscles (mBAMs) generated tetanic (active) forces upon electrical stimulation measured with a novel image-based motion detection system. mBAM myofiber hypertrophy and active force increased in response to insulin-like growth factor 1. In contrast, mBAM deterioration and weakness was observed with a cholesterol-lowering statin. The results described in this study demonstrate the integration of tissue engineering and biomechanical testing into a single platform for the screening of compounds affecting muscle strength.

Muscle Nerve **37:** 438–447, 2008

DRUG-SCREENING PLATFORM BASED ON THE CONTRACTILITY OF TISSUE-ENGINEERED MUSCLE

HERMAN VANDENBURGH, PhD,[1,3] JANET SHANSKY, MS,[1] FRANK BENESCH-LEE, BE,[3] VICTORIA BARBATA, BA,[3] JONATHAN REID,[3] LIEVEN THORREZ, PhD,[1] ROBERT VALENTINI, MD, PhD,[3] and GREGORY CRAWFORD, PhD[2]

[1] Department of Pathology, RISE Research Building, Brown Medical School/Miriam Hospital, 14 Third Street, Providence, Rhode Island 02906, USA
[2] Brown University Division of Engineering, Providence, Rhode Island, USA
[3] Myomics, Inc., Providence, Rhode Island, USA

Accepted 28 September 2007

Current high-throughput drug screening (HTS) using single-readout two-dimensional (2D) cell-based assays has contributed significantly to the identification of potential new drugs, but the assay does not completely mimic the in vivo complexity of three-dimensional (3D) tissues. The 2D assays are primarily focused on specific targets or individual biochemical pathways. For example, a 2D cell-based assay for skeletal muscle hypertrophy–inducing compounds is based on elevated expression of a single gene, the myosin heavy chain gene.[4] Another 2D cell-based assay screen for compounds that might attenuate muscle atrophy or weakness in Duchenne muscular dystrophy (DMD) is based on the increased expression of an individual cytoskeletal protein, utrophin, a potential substitute for the defective dystrophin protein.[2] Increased myofiber size (hypertrophy) is a common 2D screening indicator of compounds that stimulate muscle growth[1,26] but myofiber size is a poor indicator of muscle strength.[11] Thus, despite the development of these 2D in vitro assays, the preferred drug screening method for DMD is still the in vivo *mdx* murine model.[9,24] This is not surprising, as skeletal muscle strength results from the complex interaction of multiple second-messenger pathways and structural proteins.[8] Thus, the effect of a compound on overall tissue function may be missed by screening for effects on only a single pathway or protein target. The search for drugs targeting muscle disease has thus been hampered by the lack of adequate in vitro physiological screening technologies.

Contractile cells, such as skeletal and cardiac muscle, are difficult to maintain long-term in 2D monolayers for physiological drug screening applications due to detachment from the plate surface as

This article includes Supplementary Material available via the Internet at http://www.mrw.interscience.wiley.com/suppmat/0148-639X/suppmat/

Abbreviations: DMD, Duchenne muscular dystrophy; DMEM, Dulbecco's modified Eagle's medium; DMSO, dimethylsulfoxide; ECM, extracellular matrix; FGM, fibroblast growth medium; HCS, high-content drug screening; HTS, high-throughput drug screening; IGF-1, insulin-like growth factor-1; μposts, microposts; mBAM, miniature bioartificial muscle; PDMS, polydimethylsiloxane; SGM, skeletal muscle growth medium

Key words: Duchenne muscular dystrophy; high-content drug screening; insulin-like growth factor-1; muscle weakness; statins

Correspondence to: H. Vandenburgh; e-mail: herman_vandenburgh@brown.edu

© 2008 Wiley Periodicals, Inc.
Published online 30 January 2008 in Wiley InterScience (www.interscience.wiley.com). DOI 10.1002/mus.20931

they become functionally active with differentiation. To avoid this problem, many approaches focus on drug effects on muscle differentiation, e.g., the fusion of myoblasts into myofibers,[12] which is more representative of new myofiber regeneration than of existing myofiber strength. Cells organized into 3D structures in vitro are often more representative of in vivo tissues than 2D monolayers,[22] and, since they are normally attached to a 3D matrix, detachment from a tissue-culture dish surface is not an issue. With recent advancements in tissue engineering it may thus be possible to develop a new generation of tissue-based high "content" drug-screening (HCS) techniques whereby a compound's effect on the physiological functioning of a tissue can be ascertained.[15] This is a particularly attractive option for muscle where changes in the key tissue function, contractility, could serve as a direct assay to determine the sum effects of a compound on all the known and unknown biochemical pathways affecting force generation. Such functional or physiological-based systems may have greater potential predictive value than other 2D screening assays in the drug discovery process.

Tissue engineering of contractile tissues from cardiac and skeletal muscle in vitro from rodent and human muscle precursor cells is well advanced. The contractile cells can be maintained under tension for weeks to months,[7,17,25] and the forces generated by these engineered tissues can be measured using electronic force transducers.[6,25,35,36] Current transducers, however, are difficult to scale down to reproducibly measure the small forces generated by miniature contractile tissues in the microwell plate format used in HTS/HCS assays. We describe a new prototype 96-well assay system of tissue-engineered skeletal muscle in which force measurements are made using a novel image-based motion detection technology. This approach provides a nondestructive and sensitive method of measuring muscle force–generation changes over long periods of exposure to drug candidates. It should be a useful tool for basic research and for identifying new drug candidates for attenuating muscle wasting as well as identifying those drugs with adverse muscle side effects.

MATERIALS AND METHODS

Myoblast Tissue Culture. Primary mouse myoblasts were isolated from 6-week-old male C3HeB/FeJ mice by standard dissection techniques, and individual myoblast clones isolated as described previously.[34] The animal protocol was approved by the Miriam Hospital Institutional Animal Care and Use Committee. The cells were expanded in skeletal growth medium [SGM, 1:1 DMEM (Gibco, Grand Island New York; #11995-040) : FGM (Cambrex, Gaithersburg Maryland; #3130) containing 20% fetal bovine serum (Gibco), 1% ITS+1 (Sigma, St. Louis Missouri) and 100 U/ml penicillin / 100 μg/ml streptomycin (p/s)] in collagen-coated 100-mm tissue culture dishes. SGM contained 2 μg/ml insulin and 400 ng/ml human fibroblast growth factor (FGF). The cells were harvested when 80%–100% confluent with 0.5 mg/ml trypsin, pelleted by centrifugation, resuspended in SGM, and used for miniature bioartificial muscle (mBAM) tissue engineering.

Tissue Engineering of mBAMs. Polydimethylsiloxane (PDMS), a silicone-based elastomeric material (Sylgard 184; Dow Corning, Midland, Michigan) was used to cast 7-mm diameter wells 6-mm deep with flexible attachment microposts (μposts) of varying diameters (300–800 μm), 4–5 mm tall, and 4 mm apart (Fig. 1A–D). Sylgard 184 is a medical-grade PDMS commonly used for in vitro tissue engineering and in vivo reconstructive surgical applications, is nontoxic to skeletal muscle cells,[29] and shows minor hysteresis (<5%) and creep when used in force-

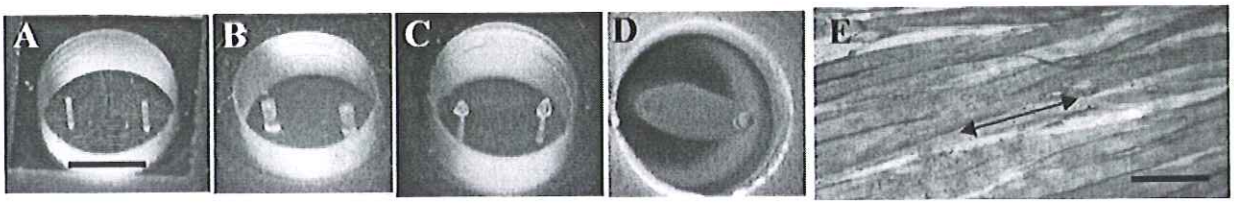


FIGURE 1. Tissue engineering mBAMs on flexible μposts. Flexible PDMS μposts were cast 4-mm apart in 7-mm diameter wells. **(A)** 165-μm radius μposts, scale bar of 4 mm; **(B)** 350-μm radius μposts; **(C)** μposts with caps for mBAM positioning at top of μposts. The caps prevent the mBAMs from sliding down the μposts or off the top when they undergo deflections; **(D)** mBAM at day 4–5 after casting in the 7-mm diameter μwell on 350-μm radius, uncapped μposts; **(E)** A 7–8-day-old mBAM whole-mount stained for sarcomeric tropomyosin (dark gray color) showing well-organized myofibers. Double-headed arrow indicates the long axis of the mBAM. Scale bar, 20 μm.

sensing applications.[23] The wells with μposts were produced in a vacuum molding process using 4–16-well Teflon molds. A second molding step created caps on the top of the flexible μposts (Fig. 1C) to help retain the mBAMs at the top of the μposts. The most critical step in reproducible casting of small-diameter μposts was complete removal of air bubbles from the PDMS by casting in a vacuum box at >30 μTorr vacuum. All casts were heat-cured at 140°C for 30 min and molds were not used for active force measurements for at least 6 days to make certain that complete polymerization had occurred. The PDMS-cast wells could be cleaned and reused at least three times with no impact on the experimental results as long as they were not exposed to the formaldehyde used to process the mBAMs for histology. mBAMs were reproducibly tissue-engineered around the caps of the μposts from the skeletal muscle cells using a modification of our previously published method for tissue engineering larger 20-mm long macro BAMs.[28,29] Briefly, mBAMs were tissue engineered by mixing proliferating myoblasts (200,000/well) with 100 μl of either ice-cold collagen–Matrigel (6 parts of 1 mg/ml rat tail collagen and 1 part of Matrigel, BD Biosciences, Bedford, Massachusetts) or fibrinogen–thrombin (0.5 mg/ml fibrinogen and 1 U/ml thrombin; Tisseel, Baxter Health Care, Westlake Village, California) in SGM and casting the mixture around the well μposts. The cell–ECM (extracellular matrix) mixture gelled rapidly at 37°C and over 24–48 h contracted away from the walls of the wells and formed around the caps on top of the μposts. The passive (resting) forces in the gel aligned the myoblasts parallel to each other in the long axis of the mBAM so that when the mBAMs were switched to differentiation medium (1:1 FGM:DMEM, 10% horse serum and penicillin-streptomycin) on day 2 postcasting, the myoblasts fused together to form parallel arrays of several hundred contractile fibers. The mBAMs were similar morphologically when formed in either fibrin or collagen extracellular matrix with aligned postmitotic muscle fibers (Fig. 1E). This is in contrast to myoblasts in 2D cultures, which form random, disorganized myofibers. mBAMs were treated with cytosine arabinoside (1 μg/ml) from day 2–5 postcasting to eliminate nonfused proliferating cells. Tissue culture media (200 μl/well) was changed daily. A 95% survival rate (continued mBAM attachment to the tops of the μposts) was obtained with these tissue culture conditions for at least 2 weeks postcasting.

mBAM Electrical Stimulation and Force Measurement. At varying times postcasting the culture wells were placed on a 37°C heating plate under a stereomicroscope (Stemi 2003; Zeiss, Thornwood, New York) with USB Digital Camera (DCM130; Madell Technology, Ontario, Canada) attachment. Platinum wire electrodes were placed in the tissue culture medium ~2 mm from each side of the mBAM. Images were captured immediately prior to electrical stimulation to determine mBAM resting force. mBAMs were then electrically stimulated to achieve maximum isotonic tetanic force (active force) by applying an electrical stimulus (QSC Amplifier; QSC Audio Products, Costa Mesa, California) of 40 V at 40 Hz with 4-ms-wide pulses for 1–2 s. Electrical stimulus parameters (voltage, frequency, duration, pulse width) were optimized in preliminary experiments. Images were captured before, during, and after electrical stimulation (3–4 frames/s) and μpost positions determined using custom LabView plug-in software and MatLab (MathWorks, Natick, Massachusetts) scripts. μPost displacement data were collected using a personal computer with data acquisition card (National Instruments, Austin, Texas). Resting and active mBAM forces were calculated based on standardized μpost deflection data obtained.

mBAM Histological Analysis. mBAMs were fixed at the end of each experiment with 2% (v/v) formaldehyde in phosphate-buffered saline for 30 min, and either whole-mount stained for fused muscle fibers using an antibody to sarcomeric tropomyosin[25] or embedded in paraffin, and longitudinal and cross-sections cut. Myofibers in sections were stained with an antibody to myosin heavy chain.[25] In both immunocytochemical staining procedures, mBAMs or cross-sections were blocked with serum, incubated with primary antibody, followed by biotinylated anti–mouse IgG and avidin-biotinylated complex coupled to horseradish peroxidase (ABC Elite Kit; Vector, Burlingame, California). Development was with 3,3′-diaminobenzidene (DAB) to produce a brown precipitate. Myofiber cross-sectional areas were measured using the interactive feature of the KS300 Image Analysis System (Zeiss) to trace the diameter of each positively stained fiber on randomly selected areas of the slides and calculate cross-sectional areas.

Myosin Isoform Analysis. Total mBAM RNA was prepared with a Ribopure kit (Ambion, Austin, Texas). Taqman gene expression assays (Applied Biosystems, Foster City, California) were used to detect the following myosin heavy chain transcripts: adult fast IId (Myh1, Mm01332489_m1), adult fast IIa (Myh2, Mm-

00454991_m1), embryonic (Myh3, Mm01332463_m1), adult fast IIb (Myh4, Mm01332518_m1), adult slow (Myh7, Mm00600555_m1), and perinatal (Myh8, Mm01329512_m1), with mouse GAPDH as an endogenous control. Reactions were performed in triplicate with Taqman one-step reverse-transcriptase polymerase chain reaction (RT-PCR) master mix (Applied Biosystems) on a 7500 Fast Real-Time PCR system (Applied Biosystems). Data analysis was performed with Sequence Detection Software v1.3.1 (Applied Biosystems) and Microsoft Excel for Mac. Expression of the different myosin heavy chain isoforms was calculated by using the delta (Ct) relative to GAPDH.

Effect of Known Drugs. *IGF-1.* Recombinant human insulin-like growth factor I (rhIGF1, Sigma) was diluted in a low serum differentiation medium (2.5% horse serum in DMEM containing penicillin-streptomycin) to a concentration of 100 ng/ml, a level shown to maximally induce BAM myofiber hypertrophy in vitro.[27]

Atorvastatin. Atorvastatin (Lipitor; Pfizer, New London, Connecticut) was suspended in DMSO at a concentration of 12.5 mM and diluted further into differentiation medium for testing on mBAMs. All atorvastatin test media, including the no-atorvastatin control medium, contained the same final concentration of DMSO (0.2% v/v or less).

For all drugs tested, mBAMs were incubated with test medium containing the specified concentration of drug beginning on day 6 or 7 postcasting, with daily media changes for the duration of each experiment. mBAMs were electrically stimulated just prior to the first addition of the drug test medium and every 1–2 days thereafter.

Statistical Analysis. Means and standard error of the means were calculated and *t*-test statistical analyses performed using SigmaStat software (Systat Software, San Jose, California), with a *P*-value less than 0.05 considered statistically significant. Power analyses were performed using GraphPad StatMate 2.00 software (San Diego, California).

RESULTS

Measurement of mBAM force generation was based on the degree of flexion of the μposts (Fig. 2A). For a μpost of radius R and length L, cast from PDMS material with a known elastic modulus (E), the moment of inertia (I) is given by $I = \frac{1}{4}\pi R^4$ and force based on μpost deflection δ by the formula: $F = 3EI\delta/L^3 = 3\pi ER^4\delta/4L^3$.[3] Since all of the parameters in the equation are known, it can be used to fit the force displacement curves using E as the only fitting parameter. μPosts of varying heights and radii were vacuum cast on a PDMS calibration platform (Fig. 2B) and μpost deflections analyzed as a measure of force with a customized displacement-force measurement device. Forces of 5 μN sensitivity could be determined with 2%–3% variability in repetitive manner since the μposts returned to their initial position after the force was released. μPosts with radii from 150–350 μm were horizontally displaced at 0.2 mm from their tops in 1–5 μm steps at a rate of 1–3 mm/min and the force required for deflection measured. The μN of measured force for the deflected μposts compared well with the values calculated from the formula for all μpost radii (Fig. 2C,D).

The mBAMs generated passive (resting) forces beginning on day 1 postcasting that were capable of flexing the μposts to different extents based on their radii. As expected, the 150-μm radius μposts were deflected to the greatest degree (Fig. 3A), with the tips of the μposts almost touching by day 4 postcasting (i.e., total μpost deflection of ~4 mm) while the 350-μm radius μposts were deflected inward by only 150–200 μm. μPosts with radii between 150 and 350 μm were deflected to intermediate amounts. The calculated resting forces generated by the mBAMs based on μpost deflections is comparable to resting forces measured previously with larger (20-mm long) macroBAMs using electronic force transducers when corrected for cell number and tissue volume.[25] The macroBAM resting force values measured with electronic force transducers indicated that the resting force plateaued around 6–10 days after BAM casting[25] and a similar result was obtained for the smaller mBAMs when measured by the μpost deflection assay (Fig. 3B). In subsequent experiments appropriate μpost radii (350–400 μm) were selected for the measurement of active tetanic forces when the mBAMs were electrically stimulated, but with minimal μpost deflection by resting tension. μPosts of 350–400 μm radius were then tested for hysteresis and creep at 37°C. With 10 repetitive deflections of 0.5 mm at 100 μm/s, mean mechanical hysteresis was 6.5% ± 1.55% (mean + SE, $n = 10$, see Suppl. Fig. 1) and creep was less than 1% after 100 deflections. Stress–strain curves for 350–400 μm radius μposts were compared for molds cast from two separate batches of PDMS and hysteresis was found to be within 1%. μPosts of this radius thus result in reproducible repetitive deflections and accurate active force measurements in response to electrical stimulation of the mBAMs could be made (see below).

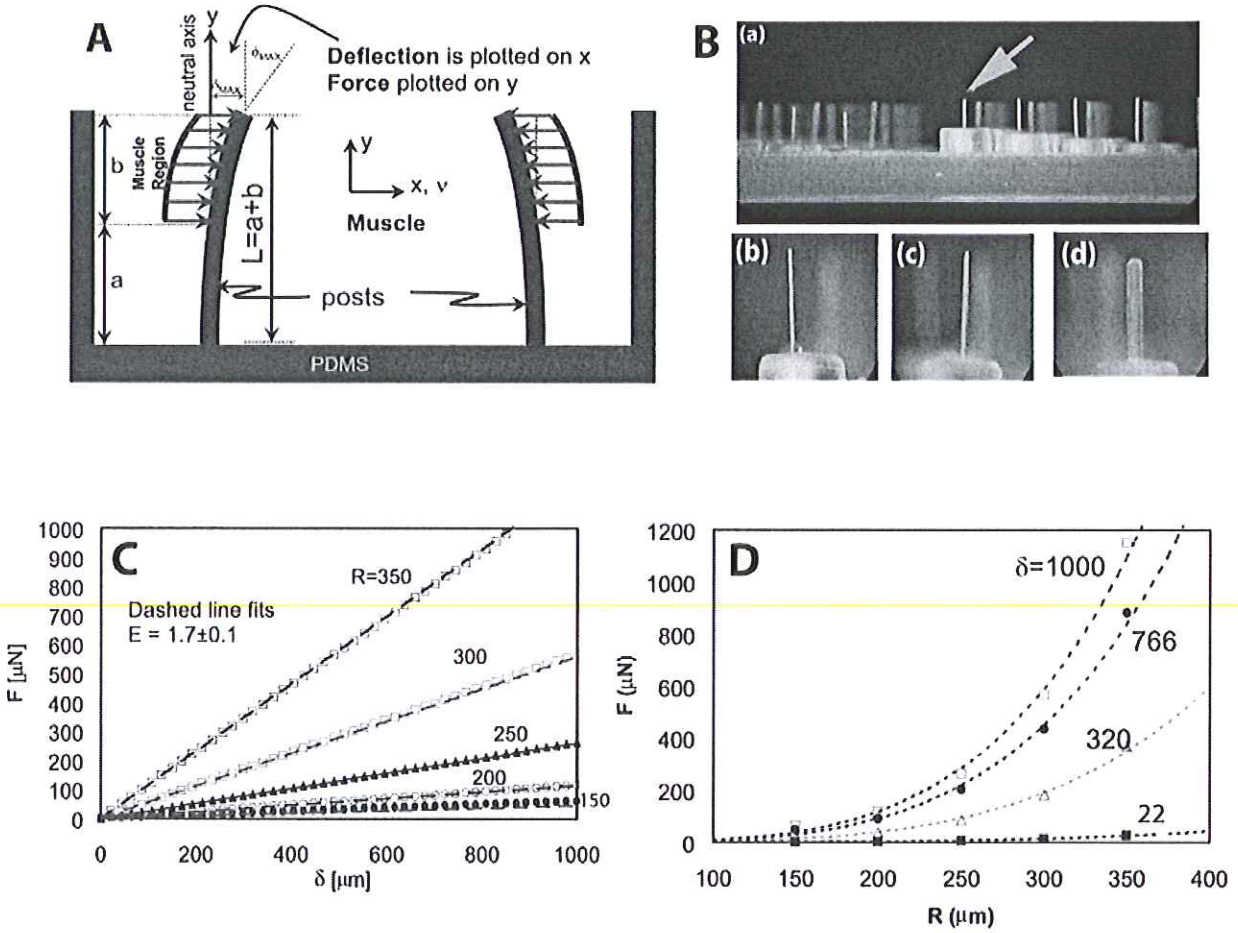


FIGURE 2. Force measurement with flexible μposts. **(A)** Mechanical model correlating μpost displacement (δ) with force (F). **(B)** A μpost calibration platform **(a)** with μposts of varying radii and lengths. The arrow indicates a μpost 100μm radius and 3.0 mm high, with the μpost height to the right going from 3.5 mm to 4.5 mm in 0.5 mm increments. **(b–d)** Enlargements of μposts of 75 μm, 150 μm, and 350 μm radius, respectively. **(C)** Force versus displacement curves. The distance of μpost deflection was determined using either an attached electronic caliper (10 μm displacement resolution) or a stereomicroscope and digital imaging motion detection system (2 μm displacement resolution). The dashed curves in the graph are fits to the above equation for μposts of 150–350 μm radii and the experimentally determined data shown with symbols. **(D)** Force vs. μpost radius curves. The μposts of varying radius were displaced by a defined distance (δ = 22, 320, 766, 1,000 μm) and the force required to deflect the μposts was measured. The symbols in the figure represent actual measurements and the dashed curves are fits to the above equation.

In preliminary experiments electrical stimulus parameters were optimized for mBAM maximal isotonic tetanic force generation (i.e., active force) based on previous studies with 20-mm-long macroBAMs (Lee et al., unpublished results), and these parameters were used in the present study (Fig. 4A, see Suppl. Video 1). mBAMs returned to their starting position within several seconds after the stimulus ended, representing a larger hysteresis for the mBAM tissue than for the PDMS μposts, as previously shown for macroBAMs.[25] Rest periods of 5–10 min between tetanic stimuli were necessary for full active force recovery (representing muscle force recovery time). Reproducible repetitive measurements could thus be performed on the same mBAMs 5–6 times when the stimuli were spaced 10 min apart. mBAMs generated increasing levels of active force when electrically stimulated as the myoblasts differentiated into organized postmitotic muscle fibers and expressed sarcomeric proteins (Fig. 4B). mBAM contraction in response to electrical stimulation was seen beginning 5–6 days postcasting, i.e., 3–4 days after switching to differentiation medium. Maximal active force of the mBAMs reached a plateau after 6–8 days postcasting and could be maintained at this level for at least another 5–7 days (Fig. 4B). Myofibers in the differentiated mBAMs expressed multiple myosin heavy chain transcripts as determined by

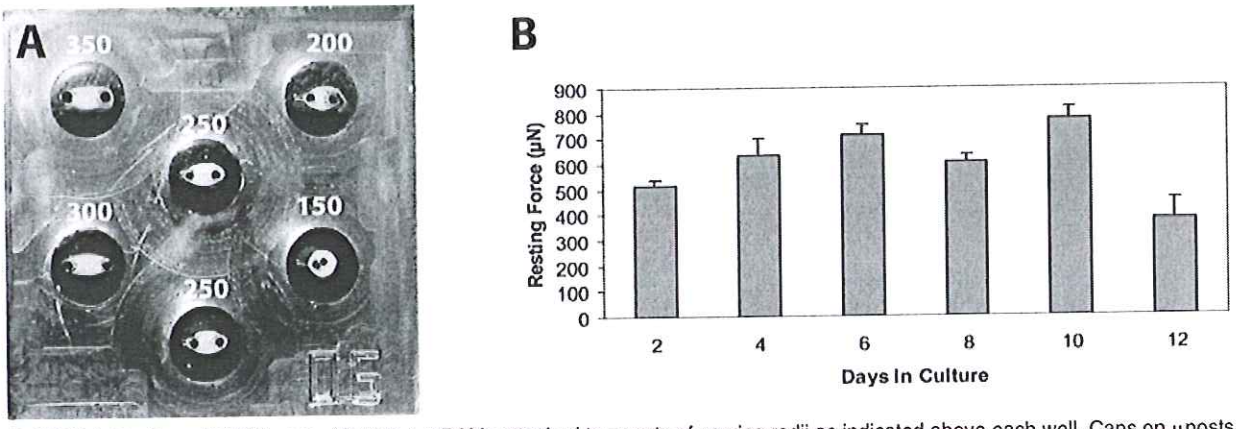


FIGURE 3. Resting mBAM Forces. **(A)** Day 4 mBAMs attached to μposts of varying radii as indicated above each well. Caps on μposts have been dyed black for better visualization of post deflections. μPosts in all the wells were the same distance apart at the beginning of the experiment. After 4 days in vitro the mBAM attached to the 150-μm posts (lower right well) has contracted to deflect the posts to a small overall distance apart, with the tips of the μposts almost touching, whereas the 350-μm μposts (upper left well) were deflected only 150–200 μm from their starting position. The caps prevented the mBAMs from sliding off the top of the μposts. **(B)** Time course of resting force generation postcasting on 4.5-mm tall μposts with a radius of 350 μm. Each bar is the mean ± SEM of four mBAMs. There was no significant difference in resting forces from day 4 to day 10 when the active forces were measured.

Q-PCR, including embryonic, perinatal, slow, fast IIb, and fast IId (Fig. 5).

To validate the μpost deflection system for potential compound screening for new drugs that increase/decrease myofiber strength, the effect of known compounds on the active force-generating ability of the mBAM postmitotic muscle fibers was examined. Active force measurements in response to compound addition were performed once the passive force had plateaued. To minimize the potential contribution of unfused myoblasts to a drug's effect, the mBAMs were preincubated for 3 days (days 2–5 postcasting) with the cell proliferation inhibitor cytosine arabinoside. Clonally derived myoblasts were also used to eliminate the potential effects of proliferating fibroblasts. Repetitive active force measurements were performed following myofiber differentiation when the

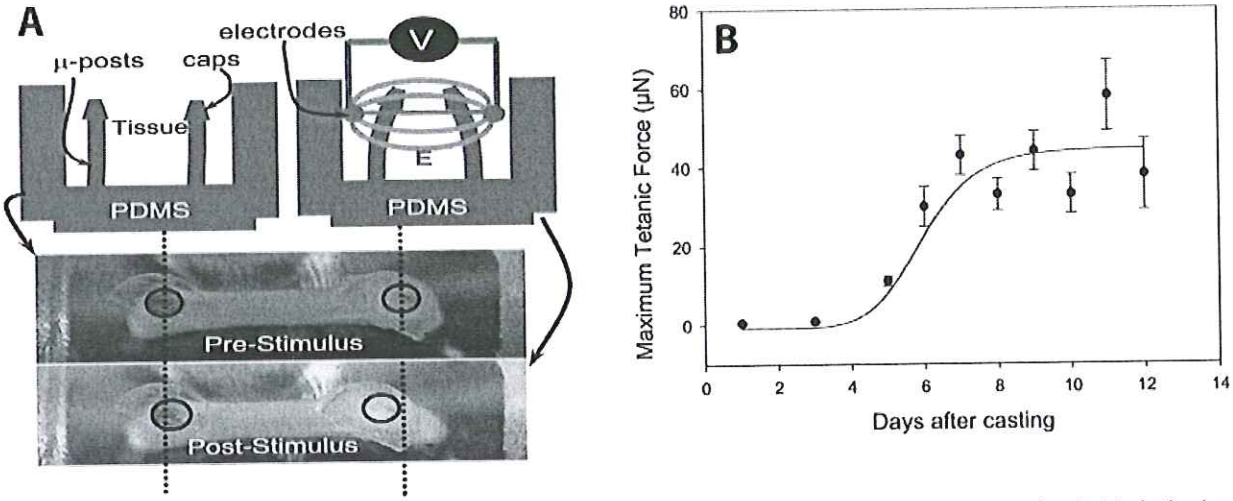


FIGURE 4. mBAM active force generation. **(A)** Example of μpost displacement in response to a maximum tetanic electrical stimulus. Prestimulus and 1-s poststimulus are shown along with simple illustrations. Circles in photographs mark the μpost top images (also see Suppl. Video 1 online). **(B)** Time course of mBAM maximum tetanic force generation with time after casting. mBAMs were electrically stimulated every 2–3 days, μpost deflection measured optically, and active force generation calculated. Results are means ± SEM from four separate experiments with n = 8–18 per timepoint. Error bars are smaller than symbols where not seen.

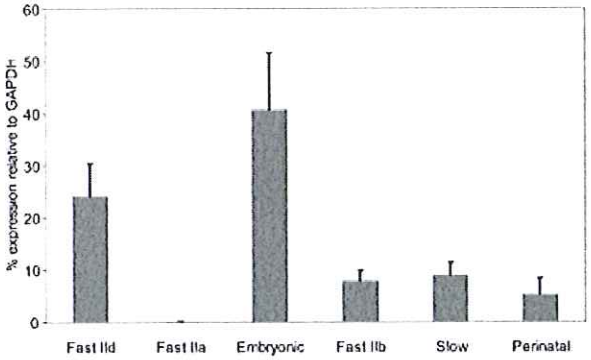


FIGURE 5. Relative myosin heavy chain isoform gene expression in mBAMs. Adult fast IId (Myh1), adult fast IIa (Myh2), embryonic (Myh3), adult fast IIb (Myh4), adult slow (Myh7), and perinatal (Myh8) were detected by quantitative PCR and expression (mean ± SEM) depicted as percent relative to GAPDH. Expression profiles represent a 12-day postcasting mBAM.

mBAM active force had plateaued (days 6–12 postcasting, Fig. 4B) so that the cumulative effects of the compound on differentiated myofiber strength/weakness could be determined.

The effect of the well-established skeletal muscle anabolic factor insulin-like growth factor-1 (IGF-1)[21] was tested first. For 2D monolayers of skeletal myofibers, incubation with 100 ng/mL IGF-1 for 3–7 days resulted in myofiber hypertrophy based on increased myofiber diameters.[27,33] IGF-1 at this concentration was found to significantly increase mean mBAM myofiber cross-sectional area by 41% after 6 days (Fig. 6A). Active mBAM force generation was significantly increased by 2 days after addition of IGF-1 to the medium and continued to increase for the next 2–4 days to levels 2–3-fold greater than control mBAMs (Fig. 6B). Similar results were obtained in a second experiment. The effect of a skeletal muscle catabolic factor was tested next. When atorvastatin was added to the mBAMs there was a concentration- and time-dependent decrease in active force generation, even at levels as low as 0.01 μM (Fig. 6C), a level close to reported circulating plasma levels for the drug. Histologically, at 0.10 μM atorvastatin caused significant myofiber necrosis (Fig. 6D). The μpost deflection system was thus able to reproducibly respond to both an anabolic and catabolic factor by an increase or decrease in active force generation, respectively.

DISCUSSION

We show that PDMS can be vacuum cast into thin flexible μposts of varying heights and diameters, with reproducible stress–strain characteristics for tissue-engineering applications. An ECM-containing cell mixture was bioengineered into contractile tissue around the caps positioned at the top of the μposts and was maintained in this position in a contractile state for several weeks. Electrical stimulation of the tissue, coupled to an imaging motion detection system that captured the μpost deflections, could be used to accurately calculate active force generated by the muscle tissue. This system thus provides a new, reproducible, nondestructive technique for active force measurements of contractile tissue-engineered constructs over extended time periods, and when coupled with the robotic technologies used for HTS provides a unique physiological assay for screening compound banks for new drugs affecting skeletal muscle strength.

Primary murine skeletal muscle myoblasts were tissue-engineered into mBAMs using standard tissue culture methods and, when differentiated into postmitotic myofibers, expressed both adult and embryonic myosin heavy chain isoforms at approximately similar levels. The percent of the adult fast myosin heavy chain transcripts was ~4-fold higher than adult slow myosin transcripts. The relative expression of the adult myosin isoforms in the mBAMs is thus similar to a 7–8-month-old adult fast murine muscle[5]; however, whereas adult fast muscle in vivo expresses only moderate levels of the embryonic myosin isoform, the mBAMs expressed a high level of this isoform (40% of the total). Thus, the noninnervated mBAM myofibers in vitro are not fully differentiated into true adult fast or slow fiber isotypes and they will likely exhibit differences in the mBAM response to anabolic/catabolic compounds compared to adult muscle in vivo. However, mBAM active force measurements are likely to be a potential useful predictor of a compound's in vivo effect on muscle fiber strength in some neuromuscular diseases.

To validate the potential of this approach for detecting compounds that affect myofiber force-generating ability, a known anabolic factor—IGF-1—was tested. IGF-1 was used in a low serum differentiation medium at a concentration previously shown to maximally induce BAM myofiber hypertrophy in vitro.[27] Myofiber diameters increased by 41% after several days of incubation while active force increased to a significantly greater extent (2–3-fold). These results are interesting since they show a clear disconnect between myofiber size increase and increased active force generation. This indicates that IGF-1 is increasing muscle force by mechanisms in addition to increased myofiber size, possibly by also increasing

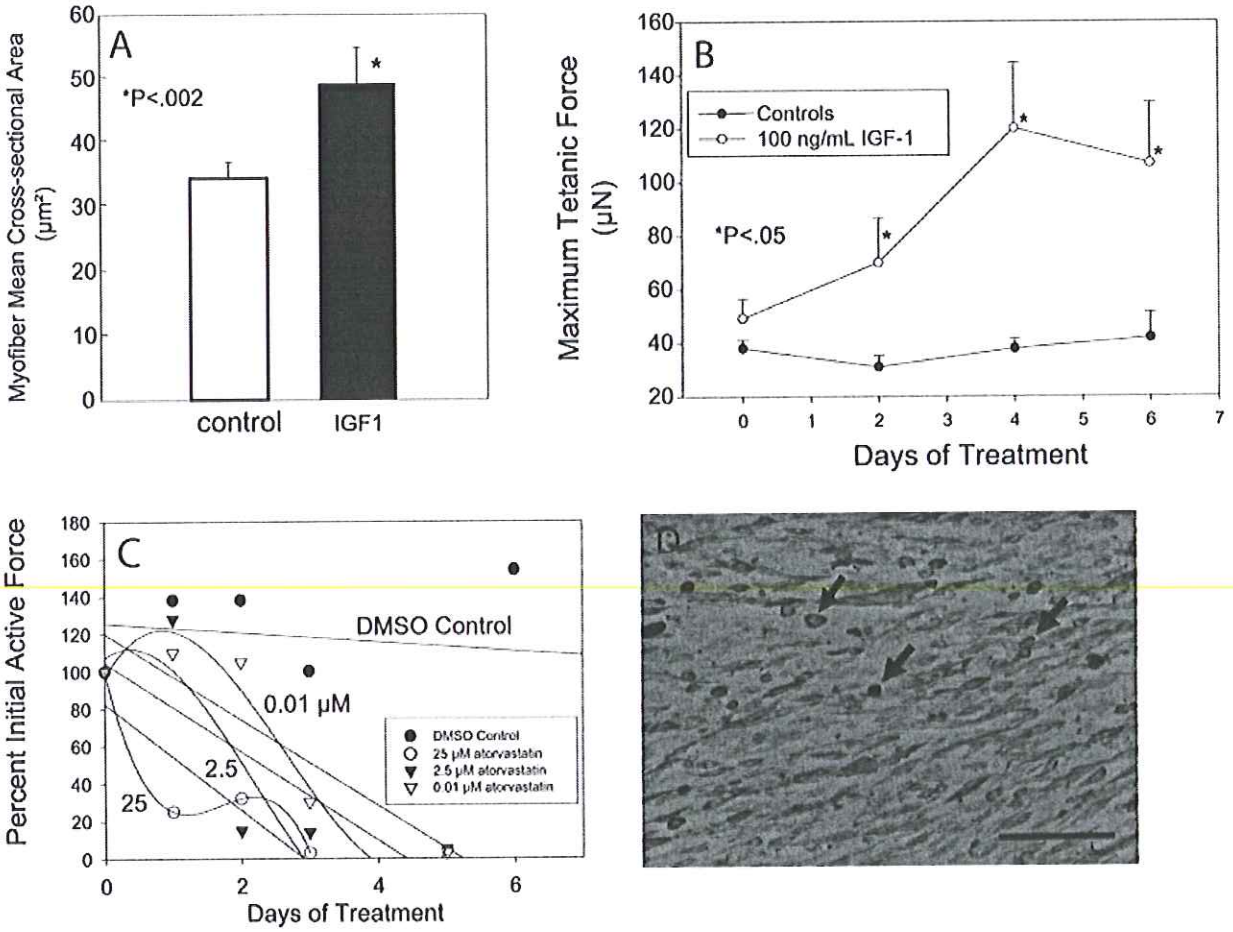


FIGURE 6. Drug-induced modulation of mBAM active force. Insulin-like growth factor-1 increased myofiber size **(A)** and active force generation **(B)**. mBAMs were allowed to differentiate for 6–7 days postcasting and then IGF-1 (100 ng/ml) was added to the wells. Values in **(A)** are the mean ± SE of 67–77 myofiber area measurements per group (n = 6 mBAMs/group). Each point in **(B)** is the mean ± SE, n = 6 mBAMs per group. **(C)** Atorvastatin decreased mBAM active force generation in a time–concentration-dependent manner. Atorvastatin at different concentrations was added to the tissue culture medium starting on day 6 postcasting. Active force was measured once every 48 h and values calculated relative to initial active force at day 6 (100%). Each point is the mean ± SE, n = 3–6 mBAMs per group and the black lines represent the cubic polynomial regression fit of the data for each concentration. **(D)** Degenerating myofibers (arrows) after exposure to 0.1 μM atorvastatin for 4–5 days. Whole-mount mBAMs were immunostained for sarcomeric tropomyosin (dark gray) similar to those in Figure 1E. Scale bar, 50 μm.

contractile protein synthesis or organization into sarcomeres.

Dose-dependent skeletal muscle pain and weakness are the main side effects of the cholesterol-lowering statins, affecting 7% of patients on statin monotherapy, and causing serious myositis and rhabdomyolysis in 0.2%–0.3% of the patient population.[31,32] Statins induce muscle weakness by unknown mechanisms, but several in vitro studies have reported adverse effects on 2D monolayers of skeletal myofibers, including histological abnormalities at 1 μM,[20] increased myofiber apoptosis at 0.5 μM,[13] and myofiber mitochondrial toxicity at 100 μM.[14] These concentrations are significantly above the serum levels found in patients on statin monotherapy.[10] Our system was used to test for potential adverse effects of atorvastatin on mBAM active force generation and histomorphometry in a concentration range more comparable to that seen in treated patients. A decrease in mBAM active force was seen within 1–3 days at high atorvastatin concentrations (2.5–25 μM) and 3–5 days at lower, more physiological levels (0.01 μM). The results reflect an advantage of using a repetitive long-term and nondestructive drug-screening assay technique such as the μpost deflection system where effects on active force-generating ability accumulate slowly over time. Also, since the time course kinetics of mBAM active force

responses to IGF-1 and the statins are different, the advantage of measuring multiple timepoints in a screening assay is evident. The statin effect is quite dramatic, with loss of almost all active force and significant histological damage to the myofibers during the time course measured. This was unexpected since atorvastatin is a relatively safe and effective drug in humans. The adverse effects found may be due to an increased sensitivity of murine muscle to statins or to the differences in the drug's pharmacokinetics and biodistribution in vitro compared to in vivo. Adverse event screening may be of particular interest for statin drugs since an increase in current recommended doses appears to have enhanced cardiovascular benefits.[30] This may require the development of modified cholesterol-lowering compounds that do not exhibit significant adverse skeletal muscle effects.[16] Our results do highlight the utility of using mBAM tissue-engineering technology as one of several in vitro screening technologies for analyzing compounds that positively or negatively affect skeletal muscle force-generating ability.

HCS screening with tissue-engineered mBAMs will be slower and more variable than current molecular, biochemical, or cell-based HTS assays because of the relatively complicated nature of the 3D engineering technology and the physiological nature of the assay; but the physiological nature of the mBAM active force assay may be more predictive of a drug's effect at the tissue level. To reduce well-to-well variability, the force-generating ability of each mBAM is measured before the addition of any test compound; thus, each mBAM serves as its own internal control. A power analysis performed on the data accumulated from experiments similar to those described in this article, where each mBAM is its own internal control, indicates that for a sample size of six wells per compound concentration, a 10% change in active force will result in statistical significance at the $P = 0.05$ level. Greater sample sizes could be utilized if smaller changes than 10%–20% are to be examined. Positive hit determination will also be enhanced by the inclusion of both positive (e.g., IGF-1) and negative (e.g., atorvastatin) controls on each 96-well plate in a random fashion, as suggested for more reliable HTS results.[19]

The current μpost deflection system can be advanced on several fronts. The results outlined in this study utilized mBAMs containing immature postmitotic murine muscle fibers without either proliferating myoblasts or fibroblasts, both of which would be significant targets for future drug screening of compounds affecting muscle strength. The myofiber only mBAMs used in the current work provide baseline data that can be followed up in future studies with the addition of proliferating myoblasts and fibroblasts to the tissue-engineering process. Similar technology can also be utilized in the future for screening tissue-culture medium or other tissue-engineering components (e.g., ECM) that stimulate the differentiation of the myofibers into more adult-like fast or slow phenotypes. Finally, the μpost deflection system can utilize primary human muscle cells (as obtained in muscle needle biopsies) as a potentially more reliable predictor than rodent primary muscle cells or muscle cell lines of a compound's effect in future clinical trials. mBAMs might also be tissue engineered from progenitor myoblasts isolated from different patient populations with various neuromuscular disorders for specific disease targeting of a potential drug. Drugs can be selected for enhancing muscle force generation to treat disorders such as the muscular dystrophies, sarcopenia of the elderly, or muscle disuse.

In summary, physiological-based HCS for muscular disease with the μpost deflection system and tissue engineering technologies may provide a new in vitro model for basic science research and for information-rich, physiologic data for future drug discovery and toxicity screening.

Supported by the Rhode Island Slater Technology Fund, NIH STTR R41 AR053386, and NSF SBIR Program Grant No. 0610721. Any opinions, findings, and conclusions or recommendations expressed in this material are those of the authors and not necessarily those of the granting agencies. Presented in abstract form at the Keystone Symposium on Tissue Engineering and Development Biology, April 2007, Snowbird, Utah.

REFERENCES

1. Bodine SC, Latres E, Baumhueter S, Lai VK, Nunez L, Clarke BA, et al. Identification of ubiquitin ligases required for skeletal muscle atrophy. Science 2001;294:1704–1708.
2. Courdier-Fruh I, Barman L, Briguet A, Meier T. Glucocorticoid-mediated regulation of utrophin levels in human muscle fibers. Neuromuscul Disord 2002;12(Suppl 1):S95–104.
3. Crandall SH, Dahl NC, Lardner TJ. An introduction to the mechanics of solids. New York: McGraw-Hill; 1999.
4. Cross-Doersen D, Isfort RJ. A novel cell-based system for evaluating skeletal muscle cell hypertrophy-inducing agents. In Vitro Cell Dev Biol Anim 2003;39:407–412.
5. Dennehey BK, Leinwand LA, Krauter KS. Diversity in transcriptional start site selection and alternative splicing affects the 5'-UTR of mouse striated muscle myosin transcripts. J Muscle Res Cell Motil 2006;27:559–575.
6. Dennis RG, Kosnik PE, Gilbert ME, Faulkner JA. Excitability and contractility of skeletal muscle engineered from primary cultures and cell lines. Am J Physiol Cell Physiol 2001;280: C288–C295.
7. Eschenhagen T, Zimmermann WH. Engineering myocardial tissue. Circ Res 2005;97:1220–1231.
8. Glass DJ. Signalling pathways that mediate skeletal muscle hypertrophy and atrophy. Nat Cell Biol 2003;5:87–90.

9. Granchelli JA, Pollina C, Hudecki MS. Pre-clinical screening of drugs using the mdx mouse. Neuromuscul Disord 2000;10: 235–239.
10. Hermann M, Bogsrud MP, Molden E, Asberg A, Mohebi BU, Ose L, et al. Exposure of atorvastatin is unchanged but lactone and acid metabolites are increased several-fold in patients with atorvastatin-induced myopathy. Clin Pharmacol Ther 2006;79:532–539.
11. Hoffman EP, Escolar D. Translating mighty mice into neuromuscular therapeutics: is bigger muscle better? Am J Pathol 2006;168:1775–1778.
12. Jiang Z, Clemens PR. Cellular caspase-8-like inhibitory protein (cFLIP) prevents inhibition of muscle cell differentiation induced by cancer cells. FASEB J 2006;20:2570–2572.
13. Johnson TE, Zhang X, Shi S, Umbenhauer DR. Statins and PPARalpha agonists induce myotoxicity in differentiated rat skeletal muscle cultures but do not exhibit synergy with cotreatment. Toxicol Appl Pharmacol 2005;208:210–221.
14. Kaufman P, Torok M, Zahno A, Waldhauser KM, Brecht K, Krahenbuhl S. Toxicity of statins on rat skeletal muscle mitochondria. Cell Mol Life Sci 2006;63:2415–2425.
15. Khademhosseini A, Langer R, Borenstein J, Vacanti JP. Tissue engineering special feature: microscale technologies for tissue engineering and biology. Proc Natl Acad Sci U S A 2006;103:2480–2487.
16. Kidd J. Life after statin patent expiries. Nat Rev Drug Discov 2006;5:813–814.
17. Kosnik PE, Dennis RG, Vandenburgh HH. Tissue engineering skeletal muscle. In: Guilak F, Butler DL, Goldstein SA, Mooney DJ, editors. Functional tissue engineering. New York: Springer; 2003. p 377–392.
18. Maganaris CN, Paul JP. Hysteresis measurements in intact human tendon. J Biomech 2000;33:1723–1727.
19. Malo N, Hanley JA, Cerquozzi S, Pelletier J, Nadon R. Statistical practice in high-throughput screening data analysis. Nat Biotechnol 2006;24:167–175.
20. Matzno S, Tazuya-Murayama K, Tanaka H, Yasuda S, Mishima M, Uchida T, et al. Evaluation of the synergistic adverse effects of concomitant therapy with statins and fibrates on rhabdomyolysis. J Pharm Pharmacol 2003;55:795–802.
21. Musaro A, McCullagh K, Paul A, Houghton L, Dobrowolny G, Molinaro M, et al. Localized Igf-1 transgene expression sustains hypertrophy and regeneration in senescent skeletal muscle. Nat Genet 2001;27:195–200.
22. Nelson CM, Bissell MJ. Of extracellular matrix, scaffolds, and signaling: tissue architecture regulates development, homeostasis, and cancer. Annu Rev Cell Dev Biol 2006;22:287–309.
23. O'Sullivan S, Nagle R, McEwen JA, Casey V. Elastomer rubbers as deflection elements in pressure sensors: investigation of properties using a custom designed programmable elastomer test rig. J Physics D Appl Phys 2003;36:1910–1916.
24. Payne ET, Yasuda N, Bourgeois JM, Devries MC, Rodriguez MC, Yousuf J, et al. Nutritional therapy improves function and complements corticosteroid intervention in mdx mice. Muscle Nerve 2006;33:66–77.
25. Powell C, Smiley B, Mills J, Vandenburgh H. Mechanical stimulation improves tissue-engineered human skeletal muscle. Am J Physiol Cell Physiol 2002;283:C1557–C1565.
26. Semsarian C, Wu MJ, Ju YK, Marciniec T, Yeoh T, Allen DG, et al. Skeletal muscle hypertrophy is mediated by a Ca2+-dependent calcineurin signalling pathway. Nature 1999;400: 576–581.
27. Shansky J, Creswick B, Lee P, Wang X, Vandenburgh H. Paracrine release of insulin-like growth factor 1 from a bioengineered tissue stimulates skeletal muscle growth in vitro. Tissue Eng 2006;12:1833–1841.
28. Shansky J, Del Tatto M, Chromiak J, Vandenburgh H. A simplified method for tissue engineering skeletal muscle organoids in vitro. In Vitro Cell Dev Biol Anim 1997;33:659–661.
29. Shansky J, Ferland P, McGuire S, Powell C, Del Tatto M, Nachman M, et al. Tissue engineering human skeletal muscle for clinical applications. In: Vunjak G, Freshney I, editors. Culture of cells for tissue engineering. Hoboken, NJ: John Wiley & Sons; 2006. p 239–257.
30. The Stroke Prevention by Aggressive Reduction in Cholesterol Levels (SPARCL) Investigators. High-dose atorvastatin after stroke or transient ischemic attack. N Engl J Med 2006; 355:549–559.
31. Thompson PD, Clarkson PM, Rosenson RS. An assessment of statin safety by muscle experts. Am J Cardiol 2006;97:69C–76C.
32. Tobert JA. Lovastatin and beyond: the history of the HMG-CoA reductase inhibitors. Nat Rev Drug Discov 2003;2:517–526.
33. Vandenburgh HH, Karlisch P, Shansky J, Feldstein R. Insulin and insulin-like growth factor-1 induce pronounced hypertrophy of skeletal myofibers in tissue culture. Am J Physiol Cell Physiol 1991;260:C475–C484.
34. Vandenburgh HH, Shansky J, Del Tatto M, Chromiak J. Organogenesis of skeletal muscle in tissue culture. In: Morgan J, Yarmush M, editors. Methods in molecular medicine: tissue engineering. Tottowa, NJ: Humana Press; 1999. p 205–217.
35. Wakatsuki T, Fee JA, Elson EL. Phenotypic screening for pharmaceuticals using tissue constructs. Curr Pharm Biotechnol 2004;5:181–189.
36. Zimmermann WH, Schneiderbanger K, Schubert P, Didie M, Munzel F, Heubach JF, et al. Tissue engineering of a differentiated cardiac muscle construct. Circ Res 2002;90:223–230.